2024 IEEE/ASME International Conference on Advanced Intelligent Mechatronics (AIM)
July 15-19, 2024. Boston, MA, USA

Cross-scan Error Evaluation of Large Size Polygon Mirror Based Laser Scanning System for Industrial 3D Printing

Bo Cong, Han Woong Yoo, Daniel Pechgraber and Georg Schitter

2024 IEEE/ASME International Conference on Advanced Intelligent Mechatronics (AIM) | 979-8-3503-5536-9/24/$31.00 ©2024 IEEE | DOI: 10.1109/AIM55361.2024.10636950

***Abstract*— This paper analyses and evaluates the cross-scan error of a large-size polygon mirror-based laser scanning system for industrial stereolithography (SLA). The polygon mirror (PM) is often used for fast scanning applications due to its superior scanning speed and large scanning angle. However, PM-based laser scanning systems are prone to cross-scan errors, restricting scanning precision. The facet tilt and scanhead dynamics are considered as two primary sources contributing to cross-scan errors. The datum-to-shaft error by manufacturing imperfections is modeled as the main cause of the facet tilts in the investigated PM-based scanner. This datum-to-shaft error varies due to radius expansion by the PM at high-speed rotations, leading to a 10 µm variation in the cross-scan error. The scanhead dynamics are measured by a vibrometer and characterized by non-deterministic vibrations and the deterministic periodic excitation. The total scanning precision of the large-size PM-based laser scanning system is approximately 160 µm mainly due to the datum-to-shaft error, limiting the precision of the PM based industrial SLA printer without any compensation.**

I. Introduction

Polygon mirror (PM) based scanning system is a popular choice for many applications, such as LiDAR [1], additive manufacture [2], [3] or laser machining [4], [5], thanks to its fast scanning speed and wide scanning angle. By rotating the PM at a high speed, PM-based scanning systems generate more than 10 times faster scanning speed in comparison to galvanometer based scanning systems of a similar scanning angle [6].

Despite the benefit in high speed and large angle, the PM-based scanning system suffers from cross-scan errors, limiting its implementation in precise scanning applications [7], [8]. Understanding the cause and demonstration of the cross-scan error is critical for the development of this technology. Based on this understanding, compensation methods such as passive correction [9] or active error compensation [10], [11] can be adopted and optimized to achieve a single digit µm scanning precision. This need becomes more evident when large-size PMs are employed, where a small angle deviation is magnified by the projection system and results in a large cross-scan error [2].

Numerous studies have investigated the causes of scanning errors for PM-based laser scanning systems. Sweeney [12] investigates a PM-based laser scanning system and provides a performance chart including cross-scan errors. A multiple reflection technique is adopted in [13] to precisely measure facet pyramidal errors of a PM. A general discussion of the causes to cross-scan errors in a PM-based scanning system is given in [7], including mounting errors of the PM to the shaft. To the best of the authors' knowledge, however few works have been conducted to analyse and quantify the mounting error of the PM as a cause of the cross-scan error. Especially, no research work has covered vibrations or mechanical deformations in the integrated PM-based laser scanning system, which can also deteriorate the scanning precision.

The contribution of this paper is the analysis and experimental evaluation of the cross-scan error including its causes of facet tilts and scannhead dynamics in a large-size PM-based laser scanning system for a high speed and high resolution industrial stereolithography (SLA) printer. The cross-scan error on the nominal scanning plane results from the laser beam deviation, and facet tilts and scanhead dynamics are raised as potential sources of this deviation. The datum-to-shaft error is raised as the main cause of the facet tilts and analysed to explain the variation of the facet tilts by the PM rotational speed, measured by an imaged-based scan line measurement system. The scanhead dynamics are quantified utilizing a vibrometer and assessed both non-deterministic vibrations and periodic motions induced by the rotating PM. An error budget is drawn from the analysis to provide indication on the achievable scanning precision without any cross-scan error compensation.

II. PM-Based Scanning System

A. System description

Fig. 1 shows a scanning system with a large-size PM, developed for a high speed and high resolution industrial SLA printer [2], and utilized for the investigation of scanning precision in this study. In the scanning system, a collimated laser beam is generated from a laser unit (PhoxX-405-300, 405 nm, Omicron-Laserage Laserprodukte GmbH, Germany), is expanded to 10 mm diameter, and is guided via optics to a polygon mirror (PLS-08-525-125-AL-7.5K, 144 mm diameter, Precision Laser Scanning LLC, United States), where it gets deflected to a maximum optical scan angle of ± 22°. The deflected laser beam is then focused by an f-theta lens (S4LFT0580/173, f=0.59 m, Sill Optics GmbH, Germany), achieving an optical resolution of approximately 30 µm with a beam scanning speed up to 460 m/s. A scanhead is a 15 mm thick aluminum plate, where the polygon scanner, the f-theta lens, and a fast steering mirror

This work was supported by FFG Basisprogramm of the Austrian BMK under Project FO999900183.

The authors are with the Advance Mechatronic System group at the Automation and Control Institute, Technische Universität Wien, A-1040 Vienna, Austria. cong@acin.tuwien.ac.at

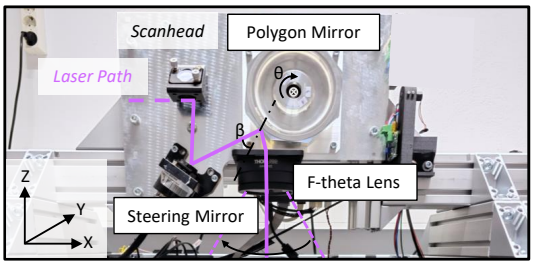

Fig. 1. Large-size PM-based laser scanning system consists primarily of an eight-facet PM, an f-theta lens and a steering mirror, all of which are integrated on the scanhead. θ represents the mechanical scanning angle of the PM, and β denotes the reflection angle of the central laser beam. The Euclidean coordinates of the scan are shown by three axes (X, Y and Z), where the X axis matches the nominal scan direction, the Y axis aligns to the PM rotating axis and Z axis is defined by the right-hand rule.

are integrated. The scanhead is tightly fixed to the printer frame.

The trade-off in optical parameters limits the design choice to a large-size PM with a long-focal-distance lens to have a scanning system with high-resolution, wide-range and high-speed [2], [12]. This choice, however, also makes the scanning system sensitive to angular errors or scanhead dynamics, hence posing challenges to achieve precise scanning.

The scanning function that describes the scanning position of the PM-based scanning system is given by

$$x = -2f\theta, \quad y = 0, \tag{1}$$

with the coordinates system shown in Fig. 1. f is the focal length of the f-theta lens and θ is the mechanical scan angle bounded by the scan range $\theta \in [-11°, 11°]$. The nominal scan direction is defined by the scanning path on the nominal scanning plane and perpendicular to the rotation axis of the PM. The scanning error is then naturally differentiated in along-scan and cross-scan directions. The cross-scan errors of the scanning system is the limiting factor for scanning precision, assuming the along-scan error is eliminated by accurate timing of laser shooting.

B. Cross-scan errors

The cross-scan errors are the deviation of scanning positions along Y direction on the nominal scanning plane, i.e. $e_{cross} = y' - y$. Fig. 2 shows a typical scanning system, where PM facet tilts and scanhead dynamics can deviate the laser beam from its nominal path, causing cross-scan errors. By adapting the scanning function (1) to facet tilts and scanhead dynamics, the caused cross-scan errors can be modelled.

The scanning function adapted to the PM facet tilt is presented in a two-steps approach. Firstly, having a tilt angle δ translates into deviations in scan directions which are described by θ' and γ.

$$\begin{aligned} \gamma &= \arcsin\left(\cos(\beta-\theta)\sin 2\delta\right), \\ \theta' &= \beta - \arctan\left(\frac{\tan(\beta-\theta)}{\cos 2\delta}\right). \end{aligned} \tag{2}$$

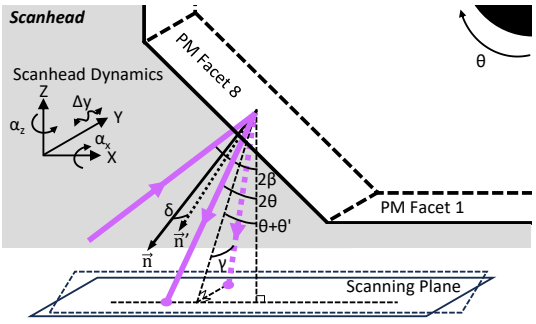

Fig. 2. Laser scanning is susceptible to geometrical errors. The nominal reflection of the laser beam is denoted with a solid-purple arrow with an optical scan angle of 2θ with respect to the central laser beam. The facet tilt, indicated by a dotted-black arrow and angle δ, deviates the laser beam from the nominal path, indicated by a dotted-purple arrow. The scanning deviation is denoted by θ' and γ. The scanhead dynamics, including translation (Δy) and rotations (α_x and α_z), alter the scanning plane (dashed frame) from the nominal scanning plane (solid frame) by moving the entire scanning system, adding to the cross-scan errors.

The PM facet tilt angle δ can be calculated by

$$\delta = \arcsin\left(\frac{\vec{n}' \cdot \vec{y}}{|n'||y|}\right), \tag{3}$$

where $\vec{n}'$ is the norm of the tilted facet, and $\vec{y}$ is a vector aligned with Y axis. Secondly, the altered laser beam is focused by f-theta lens on the scanning plane with the position in Y direction defined by

$$y'_{ft} = f \arcsin\left(\sqrt{\sin^2\gamma + \sin^2(\theta'+\theta)\cos^2\gamma}\right)\sin\psi, \tag{4}$$

where

$$\psi = \arctan\frac{\sin\gamma}{\cos\gamma\sin(\theta+\theta')}.$$

The scanning function accommodating scanhead dynamics can be approximated by

$$y'_{sd} \approx h\sin(\alpha_x) - 2f\theta\sin(\alpha_z) + \Delta y \tag{5}$$

in Y direction, where h is the distance between the scanhead and the nominal scanning plane. α_x, α_z and Δy are three decoupled motions from the scanhead dynamics, as indicated in Fig. 2. The rotation with respect to Y axis and movement in X an Z directions are not considered since their contribution to cross-scan errors is negligible.

The total cross-scan error is the sum of both error contributions resulted from (4) and (5). The standard deviation of the cross-scan error $\sigma(e_{cross})$ is adopted to represent the cross-scan error for multiple scan lines given the same reference, which also defines the cross-scan precision of the PM-based laser scanning system. The cross-scan precision, including impact from both the facet tilts and the scanhead dynamics, is estimated by

$$\sigma(e_{cross}) \approx \sqrt{\sigma^2(e_{cross}(\delta)) + \sigma^2(e_{cross}(\alpha_x, \alpha_z, \Delta y))}, \tag{6}$$

given the assumption that the two causes are independent. $e_{cross}(\delta)$ and $e_{cross}(\alpha_x, \alpha_z, \Delta y)$ denote the cross-scan errors calculated from (4) and (5) respectively.

Published version of the article: Bo Cong, Han Woong Yoo, Daniel Pechgraber and Georg Schitter, "Cross-scan Error Evaluation of Large Size Polygon Mirror Based Laser Scanning System for Industrial 3D Printing," *Proceedings of 2024 IEEE/ASME International Conference on Advanced Intelligent Mechatronics (AIM)*pp. 290–295, 2024. DOI: 10.1109/AIM55361.2024.10636950

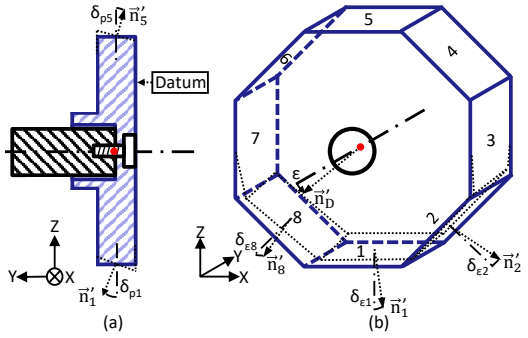

Fig. 3. PM facet tilt. (a) pyramidal errors of facet 1 and 5, denoted by δ_{p1} and δ_{p5} respectively, give facet tilt angles with respect to the PM axis (indicated by dotted lines) (b) datum-to-shaft error ε is the angle between the shaft and the datum norm $\vec{n}'_D$ of the PM (dotted arrows), which induces tilts to each facets with the sensitivity defined by (8). The example impact is visualized on facet 1,2 and 8 of the PM by dotted lines, and denoted by $\delta_{\varepsilon 1}$, $\delta_{\varepsilon 2}$ and $\delta_{\varepsilon 8}$, respectively.

III. PM Facet Tilt

PM facet tilt can have multiple physical causes such as pyramidal error of the PM or imperfect alignment between PM and shaft. Given the large size of the scanning system, 1 µrad facet tilt approximately leads to a cross-scan error of 1.2 µm in magnitude, estimated by (4).

A. Pyramidal error and datum-to-shaft error

Pyramidal error is a manufacture imperfection of the PM, where the facets are machined non-parallel to the PM central axis, as shown by δ_{p1} and δ_{p5} for the facet 1 and 5 in Fig. 3(a). Typical range of the pyramidal error is from tens to hundreds of µrad [7], and it is normally inconsistent for each facets.

Datum-to-shaft error is another primary contributor to the PM facet tilt, which can be introduced either in manufacturing or mounting of the PM. Fig. 3(b) gives a demonstration of the datum-to-shaft error ε, where each facet is affected differently. For a PM with the datum norm $\vec{n}'_D$ defined by

$$\vec{n}'_D = \left[\varepsilon_x, \sqrt{1-\varepsilon_x^2-\varepsilon_z^2}, \varepsilon_z\right] \cdot \begin{bmatrix}\vec{x}\\ \vec{y}\\ \vec{z}\end{bmatrix}, \tag{7}$$

the tilt of each PM facet is approximated by a sensitivity matrix

$$\begin{bmatrix}\delta_{\varepsilon 1}\\ \delta_{\varepsilon 2}\\ \delta_{\varepsilon 3}\\ \vdots\\ \delta_{\varepsilon 8}\end{bmatrix} \approx \begin{bmatrix}\sin 0 & -\cos 0\\ \sin\frac{2\pi}{8} & -\cos\frac{2\pi}{8}\\ \sin\frac{4\pi}{8} & -\cos\frac{4\pi}{8}\\ \vdots & \vdots\\ \sin\frac{2\pi 7}{k} & -\cos\frac{7\pi}{8}\end{bmatrix} \cdot \begin{bmatrix}\varepsilon_x\\ \varepsilon_z\end{bmatrix}, \tag{8}$$

with ε_x and ε_z of small magnitude. $\delta_{\varepsilon k}$ denotes the facet tilt of the facet k, caused by the datum-to-shaft error ε,

$$\varepsilon = \arcsin\left(\sqrt{\varepsilon_x^2+\varepsilon_z^2}\right) \approx \sqrt{\varepsilon_x^2+\varepsilon_z^2}. \tag{9}$$

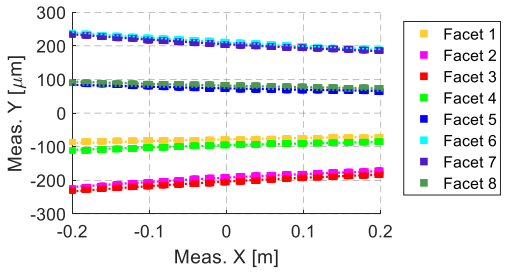

Fig. 4. Measured cross-scan error with the PM rotating 7500 RPM. The scan lines are measured at multiple sections over the scan range, depicted by colour-coded squares, with $\sigma(e_{cross})$ = 157 µm for 8 facets. The scan lines estimated from facet tilts are plotted with dotted lines, with discrepancy less than 1.5 μm_{RMS} referred to the measurement.

TABLE I
Estimated facet tilt of the PM in µrad.

Facet	1	2	3	4	5	6	7	8
δ	-83	-203	-215	-101	78	222	217	86
δ_ε	-82	-211	-216	-95	82	211	216	95
δ_p	-1	8	1	-6	-4	11	0	-9

The total facet tilt is the sum of the impact from the pyramidal error and the datum-to-shaft error,

$$\delta = \delta_p + \delta_\varepsilon.$$

B. Cross-scan precision and angle estimation

The facet tilt angles caused by both the pyramidal error and the datum-to-shaft error are repetitive with every PM revolutions as each facet is sequentially and repetitively engaged for scanning the laser beam. Given this characteristic, the cross-scan error from each facet can be measured using an image-based scan line measurement system [2]. This measurement system captures multiple images of the scan line, using a CMOS camera, at multiple locations within the scanning range, to extract the deterministic cross-scan error from each PM facets. Fig. 4 shows the measurement results of the scan lines by all 8 facets, with a cross-scan precision $\sigma(e_{cross})$ = 157 µm.

By fitting the scanning function (4) to the measurement, the cross-scan error caused by facet tilts can be estimated, shown by dotted lines in Fig. 4. The corresponding tilt angle δ of each PM facet is provided in Table I. The discrepancy between the measured cross-scan error and the estimated error from facet tilts attributes to other periodic error sources, such as scanhead dynamics.

The contribution to facet tilt from the datum-to-shaft error δ_ε can be extracted by computing the minimum norm solution for the linear equation (8), and the corresponding datum-to-shaft error ε is revealed as

$$\varepsilon = 231\,\mu\text{rad}, \quad [\varepsilon_x, \varepsilon_z] = [-216, 82] \times 10^{-6}. \tag{10}$$

Based on this estimation of δ_ε, the pyramidal error contributed facet tilt δ_p is calculated from the difference between δ and δ_ε for each PM facet. The resulted facet tilts from both causes are listed in Table I.

Published version of the article: Bo Cong, Han Woong Yoo, Daniel Pechgraber and Georg Schitter, "Cross-scan Error Evaluation of Large Size Polygon Mirror Based Laser Scanning System for Industrial 3D Printing," *Proceedings of 2024 IEEE/ASME International Conference on Advanced Intelligent Mechatronics (AIM)*pp. 290–295, 2024. DOI: 10.1109/AIM55361.2024.10636950

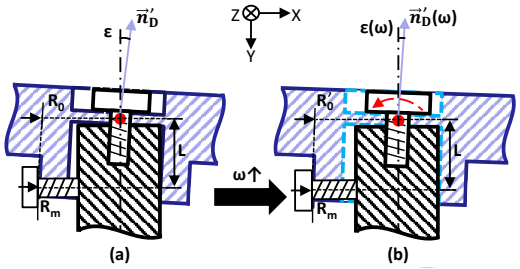

Fig. 5. PM mount and its variation. (a) the PM is screw-mounted radially and axially to the shaft. The stress induced deformation results in a datum-to-shaft error, indicated by ε. (b) by rotating the PM to a high speed ω, centrifugal stress expands the PM radially and changes the datum-to-shaft error, indicated by $\varepsilon(\omega)$.

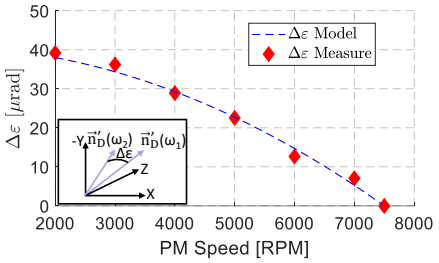

Fig. 6. Datum-to-shaft error variation $\Delta\varepsilon$ over different PM rotational speeds. Taking the datum-to-shaft error at 7500 RPM as a reference, the error variation predicted by the annular disk model is plotted in a dashed-blue line. The error variation estimated from the cross-scan error measurement is marked with red ♦.

C. PM Facet Tilt Variation

The PM mounting error, as one of the causes to datum-to-shaft error, is susceptible to the PM rotational speed, which can lead to a PM facet tilt variation.

In the PM-based scanning system, the PM is screw-mounted onto the shaft in both radial and axial directions. As screw mounts require mechanical stress between parts to secure the fixation, it unavoidably induces deformation on the parts. Fig. 5(a) shows a concept diagram of the PM mount in the designed scanning system, and the deformation caused by mounting stress. Given the deformation, a datum-to-shaft error is formed in the scanning system, which can be estimated by

$$\varepsilon = \arctan\left(\frac{-R_0+R_m}{L}\right) \approx \frac{-R_0+R_m}{L}. \tag{11}$$

R_0 and R_m denote the radius of the mounting location with respect to the PM center and the shaft center. L indicates the distance between the axial fixation and the radial fixation.

By rotating the large PM at a high speed, large centrifugal stress is applied on the mirror structure and leads to a radial expansion of the PM, shown in Fig. 5(b). As results, the datum orientation of the PM is varied to accommodate the expansion. The inner radius expansion of the rotating PM is estimated by a homogeneous annular disk model [14],

$$R_0' = \frac{\rho\omega^2 R_0}{4E}\left[(3+\nu)R_1^2 + (1-\nu)R_0^2\right], \tag{12}$$

with inner and outer diameter matched with the PM, denoted by R_0 and R_1, respectively. ρ, E and ν are the density, elastic modulus and Poisson's ratio of the PM, respectively. ω denotes the rotational speed of the PM in rad/s. As the radial expansion of the shaft is negligible compared to the PM, the variation of the datum-to-shaft error $\Delta\varepsilon$ for a PM rotational speed change can be predicted simply by

$$\Delta\varepsilon = \frac{R_0' - R_0}{L}, \tag{13}$$

with R_0' calculated from (12). Fig.6 shows the predicted datum-to-shaft error variation with the reference condition as the PM rotates 7500 revolutions per minute (RPM).

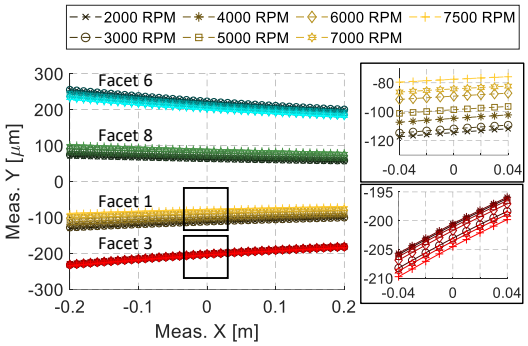

Fig. 7. Cross-scan error variation over different PM rotational speed. The measurement fitted scan lines of facet 1,3,6, and 8 are plotted as examples to demonstrate the impact of varying rotational speed (indicated by markers) on cross-scan errors. For facet 1, more than 30 μm error change is observed, while less than 5 μm is measured for facet 3. The cross-scan precision $\sigma(e_{cross})$ ranges from 157 μm to 167 μm for the tested PM rotational speeds.

D. Cross-scan precision variation

Using the same image-based measurement system as in Section III-B, the scan lines can be retrieved over different PM rotational speeds. Fitting the measured scan lines to the scanning function (4), Fig. 7 shows the cross-scan error due to facet tilts for the rotational speed from 2000 to 7500 RPM.

The scan line of each PM facet shows different magnitudes of variation by increasing the rotational speed. The largest variation is observed with facet 1, where more than 30 μm cross-scan error changes are measured. When the PM is rotating 7500 RPM, a cross-scan precision $\sigma(e_{cross})$ of 157 μm is evaluated for the scanning system. As the rotational speed decreases to 3000 RPM, the cross-scan precision is deteriorated to 167 μm. Despite the variation driven by PM rotational speeds, a significant amount of cross-scan errors remain unchanged. This portion attributes most likely to the static facet tilt, yielded from manufacturing errors.

The datum-to-shaft error of each rotational speed $\varepsilon(\omega)$ can be extracted from the measured cross-scan errors and the $\Delta\varepsilon$ is estimated from the measurement by

$$\Delta\varepsilon \approx \sqrt{(\varepsilon_x(\omega_1)-\varepsilon_x(\omega_2))^2 + (\varepsilon_z(\omega_1)-\varepsilon_z(\omega_2))^2}. \tag{14}$$

Published version of the article: Bo Cong, Han Woong Yoo, Daniel Pechgraber and Georg Schitter, "Cross-scan Error Evaluation of Large Size Polygon Mirror Based Laser Scanning System for Industrial 3D Printing," *Proceedings of 2024 IEEE/ASME International Conference on Advanced Intelligent Mechatronics (AIM)*pp. 290–295, 2024. DOI: 10.1109/AIM55361.2024.10636950

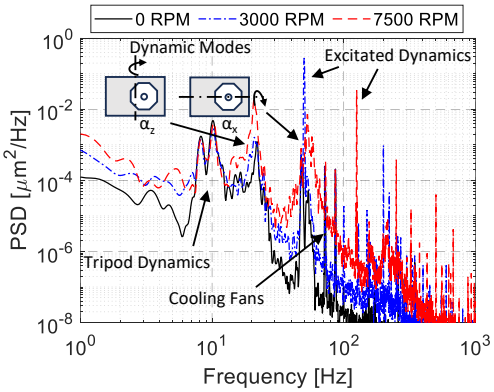

Fig. 8. PSD of vibrations in scanhead. The solid-black line describes the vibration transmitted to the scanhead when the PM is static (0 RPM). The dash-dotted blue and dashed-red line show the vibration level when the PM is rotating 3000 and 7500 RPM, respectively.

The measurement based estimation on $\Delta\varepsilon$ is plotted against the model predictions in Fig. 6, with mismatch less than 1.4 µrad. The maximum datum-to-shaft error change is 39 µrad for PM rotational speeds from 2000 to 7500 RPM.

IV. Scanhead Dynamics

The scanhead dynamics can be critical for a large-size scanning system as the cross-scan errors due to the scanhead rotations increases proportionally by the focal length. Given the large-size PM rotating at a high speed, a small misalignment of the shaft results in an unbalanced force, causing significant increase of vibrations [15], [16]. Moreover, the periodic force from rotating PM exerts onto the scanhead and triggers dynamic motions at the same frequency [16]. The scanhead vibration can cause non-deterministic scanning errors while the excited motions are generally synchronized with the excitation in a deterministic and periodic manner.

A. Vibration increment

The vibration of the scanhead is measured at multiple locations on the front side of the scanhead with a vibrometer (OFV-534, Polytec GmbH, Germany) mounted on a tripod, positioned approximately 0.5 m away from the scanhead. The vibration, measured close to the PM, is plotted in power spectral density (PSD) in Fig. 8.

The tripod modes (8 Hz and 10 Hz) and cooling fan noises are identified in the measured PSD. Two structural resonances of the scanhead can be seen at approximately 21 Hz and 55 Hz, corresponding to the rotation α_z and α_x, respectively. Likely, due to stiff connections between the scanhead and the frame, the vibration increase is constrained to an amplitude less than 0.02 µm²/Hz in the PSD. The dynamics excited by PM rotations are distinctively visible at 50 Hz and 125 Hz for the rotational speed of 3000 and 7500 RPM respectively, as well as the higher order harmonics. The increase of PM rotational speed lifts the level of vibration, and this increment is especially apparent at the frequency

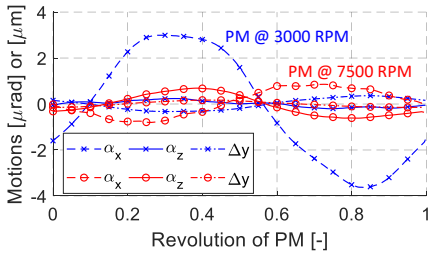

Fig. 9. Periodic motions of the scanhead with the PM rotating 3000 RPM (blue ×) and 7500 RPM (red ○). The scanhead rotation α_x (dashed lines) is dominant over α_z (solid lines) and Δy (dash-dotted lines), which has a peak-to-peak amplitude of 6.6 µrad and 1.7 µrad for the two evaluated rotational speeds.

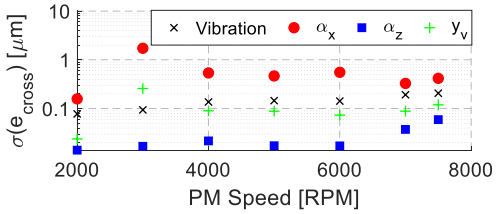

Fig. 10. Cross-scan error caused by the scanhead dynamics. The rotation around X axis contributes the largest amount to the cross-scan error.

range close to the structural resonance. The vibration, excluding the periodic motions, is evaluated of 0.07 µm, 0.09 µm and 0.21 µm for PM with 0, 3000 and 7500 RPM rotational speed, respectively.

B. Periodically excited dynamics

The periodically excited dynamics can be extracted by synchronizing the vibrometer measurements of multiple locations with the PM revolution. By averaging the measurement over multiple revolutions, the repetitive motions of α_x, α_z and Δy are discovered and plotted in Fig. 9.

The second structural mode of the scanhead, being the rotation around X axis, is amplified significantly by PM rotating 3000 RPM, equivalent to an excitation frequency of 50 Hz. This excitation frequency coincides with the resonance frequency of the structural mode, and triggers a periodic rotation of 6.6 µrad peak-to-peak amplitude. The periodic motions of α_x, α_z and Δy exhibit mostly the first harmonic of the excitation frequency.

C. Impact on cross-scan precision

The scanhead vibration is treated as non-deterministic error, mapped to the cross-scan error, and the impact from the periodic motions is estimated using the scanning function (5). Fig.10 summarizes the estimated cross-scan errors for different PM rotational speeds.

The periodic rotation α_x has the largest impact on the cross-scan precision with the maximum contribution of 1.7 µm. The total impact on the precision from the scanhead dynamics is estimated by the quadratic sum of the total

Published version of the article: Bo Cong, Han Woong Yoo, Daniel Pechgraber and Georg Schitter, "Cross-scan Error Evaluation of Large Size Polygon Mirror Based Laser Scanning System for Industrial 3D Printing," *Proceedings of 2024 IEEE/ASME International Conference on Advanced Intelligent Mechatronics (AIM)*pp. 290–295, 2024. DOI: 10.1109/AIM55361.2024.10636950

TABLE II
BUDGET ANALYSIS OF CROSS-SCAN ERROR ($\sigma(e_{cross})$ [μm])

PM Rot. Speed	2000 *RPM*	3000 *RPM*	4000 *RPM*	5000 *RPM*	6000 *RPM*	7000 *RPM*	7500 *RPM*
Facet Tilts							
Pyra.*	4.6	4.6	4.6	4.6	4.6	4.6	4.6
Datum	165.9	166.4	162.5	160.9	158.4	158.2	157.0
Sum	166.0	166.6	162.5	161.0	158.5	158.3	157.2
Scanhead Dynamics							
Vibration	0.1	0.1	0.1	0.1	0.1	0.2	0.2
Periodic	0.1	1.4	0.4	0.4	0.5	0.2	0.4
Sum	0.1	1.4	0.4	0.4	0.5	0.3	0.4
Total Cross-scan Error (No compensation)							
Total	166.0	166.6	162.5	161.0	158.5	158.3	157.2

**The average value of the pyramidal error, derived by all tested PM rot. speeds.*

periodic impact and the vibration, which is less than 1.4 µm for all tested PM rotational speeds.

V. BUDGET ANALYSIS OF CROSS-SCAN ERROR

The total cross-scan error is estimated by the quadratic sum of the error caused by the facet tilt and the scanhead dynamics as they are independent. For the facet tilt, the pyramidal error and datum-to-shaft error are added linearly before applying to the scanning function to calculate the induced cross-scan error. For the scanhead dynamics induced errors, the periodic contributions (from α_x, α_z and Δy) are added up linearly and then summed quadratically with the vibration induced errors. The resulted standard deviations of cross-scan error are summarized in Table II.

The most cross-scan error results from the facet tilt, limiting the large-size PM-based scanning system by approximately 160 µm scanning precision. The scanhead dynamics is largely suppressed by the rigid connection to the frame, leaving less than 1.4 µm impact to the cross-scan precision. Considering the optical resolution of 30 µm, the PM-based scanning system is mainly limited by the PM facet tilt. To improve the scanning precision, the PM facet tilt has to be compensated by either passive or active methods [9], [10]. An active error compensation (AEC) method is demonstrated to compensate for PM facet tilts with a fast steering mirror (FSM) [11]. An advanced AEC based on iterative learning control achieves a 23 µm peak-to-peak scanning precision by compensating for the cross-scan error induced by facet tilts and periodic scanhead motions while it is evaluated only for a single PM rotational speed [2]. Calibration procedures can be devised for the datum-to-shaft error variation to further improve the AEC.

By the evaluation of cross-scan errors in the PM-based laser scanning system, the proposed datum-to-shaft error is revealed as the largest contributor with approximately 160 µm scanning precision and even varies by PM rotational speeds, limiting the precision of the PM based industrial SLA printer without any cross-scan error compensation.

VI. CONCLUSION

In this paper, the cross-scan error caused by PM facet tilts and scanhead dynamics are evaluated for a large-size PM-based laser scanning system for a industrial 3D printer. The facet tilt, including contribution from the pyramidal error and the datum-to-shaft error, leads to a standard deviation of the cross-scan error about 160 µm. Additionally, variation of the PM datum orientation occurs up to 39 µrad due to the radius expansion of the PM by high-speed rotations, leading to a 10 µm variation in the cross-scan error. The scanhead dynamics are characterized by vibrations and the periodic motions, adding together 1.4 µm to the total scanning precision. Without any compensation, the achieved scanning precision of the large-size PM-based laser scanning system is approximately 160 µm, mainly limited by the datum-to-shaft error. This result also shows that the cross-scan error compensation is essential for high resolution high speed PM based laser scanning system to maintain the designed optical resolution of 30 µm.

The developed analysis of the cross-scan error can be used to enhance PM-based laser scanning systems for industrial 3D printing and many other applications such as LiDAR and laser machining. For example, methods for mounting the PM to the shaft can be improved to reduce the risk of a large datum-to-shaft error, and AEC can be extended for various PM rotational speeds by the radius expansion model.

REFERENCES

[1] T. Raj, F. H. Hashim, A. B. Huddin, M. F. Ibrahim, and A. Hussain, "A survey on lidar scanning mechanisms," *Electron.*, vol. 9, no. 5, p. 741, Apr. 2020.
[2] B. Cong, H. W. Yoo, D. Pechgraber, and G. Schitter, "Advanced active error compensation for polygon mirror based stereolithography," *IEEE Trans. Ind. Electron.*, under review.
[3] H. Choi and W.-C. Kim, "Design of polygonal mirror-based laser scanning optics for fast & highly precise stereolithographic apparatus," *J. Mech. Sci. Technol.*, vol. 36, no. 2, pp. 835–844, Feb. 2022.
[4] F. Roessler and A. Streek, "Accelerating laser processes with a smart two-dimensional polygon mirror scanner for ultra-fast beam deflection," *Adv. Opt. Technol.*, vol. 10, no. 4–5, pp. 297–304, Jul. 2021.
[5] K. van der Straeten, O. Nottrodt, M. Zuric, A. Olowinsky, P. Abels, and A. Gillner, "Polygon scanning system for high-power, high-speed microstructuring," *Procedia CIRP*, vol. 74, pp. 491–494, 2018.
[6] R. P. Aylward, "Advanced galvanometer-based optical scanner design," *Sens. Rev.*, vol. 23, no. 3, pp. 216–222, Sep 2003.
[7] G. F. Marshall and G. E. Stutz, Eds., *Handbook of Optical and Laser Scanning*. CRC Press, Oct 2018.
[8] V.-F. Duma and J. P. Rolland, *Mechanical Constraints and Design Considerations for Polygon Scanners*. Springer Netherlands, 2010, pp. 475–483.
[9] J. M. Tamkin, "Evolution of catadioptric scan optics for wide-field high-resolution applications," in *Proc. SPIE 5873*, Aug 2005.
[10] J. Wu and M.-H. Chu, "Wobble error correction for laser scanners," in *Proc. SPIE*, A. G. Tescher, Ed. SPIE, dec 1986.
[11] B. Cong, J. Schlarp, and G. Schitter, "Iterative learning control for the active error correction of polygon mirror based laser scanning," in *2022 IEEE/ASME Int. Conf. on Adv. Intel. Mechatron.(AIM)*, Jul 2022.
[12] M. N. Sweeney, "Polygon scanners revisited," in *SPIE Proceeding 3131: Optical Scanning Systems: Design and Applications*, Jul 1997.
[13] M. Arif Sanjid and K. P. Chaudhary, "A novel multiple reflections technique to calibrate polygons and evaluation of its uncertainty of measurement," *MAPAN*, vol. 26, no. 1, pp. 29–35, Mar. 2011.
[14] W. C. Young, R. G. Budynas, and A. M. Sadegh, *Roark's formulas for stress and strain*. McGraw-Hill Education, 2012.
[15] A. Sekhar and B. Prabhu, "Effects of coupling misalignment on vibrations of rotating machinery," *J. Sound Vib.*, vol. 185, no. 4, pp. 655–671, Aug. 1995.
[16] O. Matsushita, M. Tanaka, H. Kanki, M. Kobayashi, and P. Keogh, *Vibrations of Rotating Machinery: Volume 1. Basic Rotordynamics: Introduction to Practical Vibration Analysis*. Springer Japan, 2017.

Published version of the article: Bo Cong, Han Woong Yoo, Daniel Pechgraber and Georg Schitter, "Cross-scan Error Evaluation of Large Size Polygon Mirror Based Laser Scanning System for Industrial 3D Printing," *Proceedings of 2024 IEEE/ASME International Conference on Advanced Intelligent Mechatronics (AIM)*pp. 290–295, 2024. DOI: 10.1109/AIM55361.2024.10636950